PCCP

PAPER

View Article Online
View Journal

Cite this: DOI: 10.1039/c9cp05527d

Dopamine oxidation at gold electrodes: mechanism and kinetics near neutral pH†

Raphael P. Bacil,[ab] Lifu Chen,[a] Silvia H. P. Serrano[b] and Richard G. Compton*[a]

Received 9th October 2019,
Accepted 20th November 2019

DOI: 10.1039/c9cp05527d

rsc.li/pccp

The two-electron electrochemical oxidation of dopamine is studied voltammetrically at gold macro-electrodes around neutral pH with simulations used to give kinetic and mechanistic data. In particular, the system shows "potential inversion" in which the thermodynamic oxidation potential of dopamine to form the corresponding semi-quinone formation occurs at a more positive potential than that of the oxidation of the semi-quinone to the quinone form. The use of Tafel slopes measured from the voltammograms as a function of the voltage scan rate is show to be a particularly sensitive indicator of mechanism showing the effect of the follow-up chemistry in which the two-electron oxidation product undergoes an irreversible cyclization reaction.

Introduction

We recently addressed the mechanism of dopamine oxidation under conditions of high acidity (pH = 0), where the overall process is described by Scheme 1 and was studied electrochemically using glassy carbon and carbon microdisk electrodes.[1] The process was revealed to be multistep with two-electron transfers, the first oxidizing dopamine, A, to the semi-quinone, B, and the second the semi-quinone to the quinone form, C and showing the phenomenon of 'potential inversion' in which the formal potential for the A/B oxidation ($E^0_{fA/B}$) was found to have a more positive value than that for the B/C oxidation, $E^0_{fB/C}$. Such inversion behaviour has also been observed in the oxidation of catechol[2] and other systems.[3,4] For catechol, a full "scheme of squares" analysis was possible.[2] The potential inversion is attributed to solvation[5] and may be generically typical of hydroquinone/quinone systems in aqueous but not non-aqueous systems.

$$A - e^- \rightleftharpoons B \quad E^0_{fA/B} \qquad (1)$$

$$B - e^- \rightleftharpoons C \quad E^0_{fB/C} \qquad (2)$$

Dopamine (DA) has an important physiological role as a neurotransmitter in the central nervous system[7,8] leading to multiple studies which, as summarized in Tables 1 and 2, have revealed that the oxidation leads to 'follow-up' chemistry in which the quinone form, C, undergoes a cyclization reaction, Scheme 2, and also polymerization.[9–13] Such chemistry is minimised at low pH values, where the thermodynamics strongly discourages the deprotonation required for a Michael type reaction within or between oxidized dopamine molecules. In terms of understanding and quantifying the kinetics and thermodynamics of the two-electron transfer processes, A/B and B/C, such follow-up chemistry produces an additional complication. On the other hand, it has been shown *via* computational simulation[14] that, when coupled to follow-up chemical reactions with sufficient fast reaction kinetics, a fast electron transfer process may appear electrochemically irreversible as judged by, in particular, Tafel analysis. Proof of concept was demonstrated experimentally with pyrylium salt reduction and

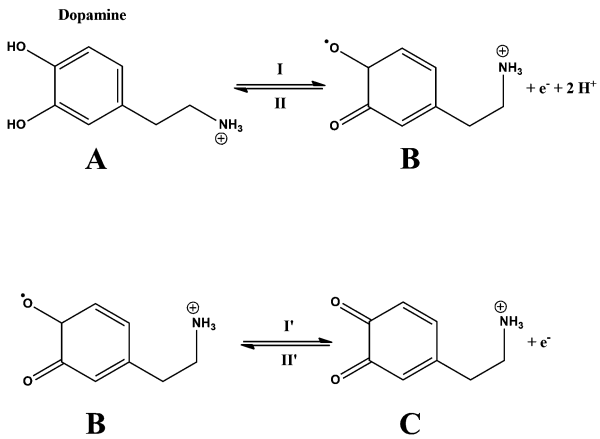

Scheme 1 Schematic representation of the literature dopamine electrochemical oxidation mechanism.[1]

[a] University of Oxford, Physical and Theoretical Chemistry Laboratory, South Parks Road, Oxford, OX1 3QZ, UK
[b] Instituto de Química, Universidade de São Paulo, Departamento de Química Fundamental, Av. Prof. Lineu Prestes, 748 - Butantã - São Paulo – SP, 05508-000, Brazil. E-mail: richard.compton@chem.ox.ac.uk; Fax: +44 (0)1865 275410; Tel: +44 (0)1865 275957

† Electronic supplementary information (ESI) available. See DOI: 10.1039/c9cp05527d

Table 1 Previous electrochemical studies of dopamine oxidation

Focus	Electrode material	Ref.
Cyclization	Carbon paste	15
Cyclization/Michael addition	Pyrolitic graphite	16
		17
Cyclization/Polymerization	Platinum	18
Cyclization	Carbon paste	19
Cyclization/Michaels addition	Carbon paste	20
Cyclization	Carbon paste	21
Michael Addition/Cyclization	Carbon paste	22
Cyclization/Polymerization	Gold	23
Cyclization/Michael addition	Glassy carbon	24
Scheme of square	Glassy carbon/carbon microdisk	1
Scheme of square	Glassy carbon/carbon microdisk	2
Scheme of square	Glassy carbon	25
Scheme of square	Carbon paste	26
Michael addition	Glassy carbon	27
Michael addition	Glassy carbon	28
Michael addition	Glassy carbon	29
Scheme of squares study/pK_a values	Gold	6
Disproportionation	Carbon fiber microdisk	30
Polymerization	Gold/Platinum/Carbon	31
Polymerization	Pyrolytic graphite	32
Dimerization/Polymerization	Gold	33
Electrosynthesis	Carbon rod	34
Neurological detection	Carbon fiber microelectrode	7

Table 2 Selected non-electrochemical studies of the oxidation of dopamine

Focus	Methodology	Ref.
Cyclization/polymerization	UV-Vis	9
Michael addition/polymerization	UV-Vis/XPS	10
Polymerization	NMR/FT-IR	11
Polymerization	Synthesis and general characterization	12
Cyclization	Theoretical calculations	13

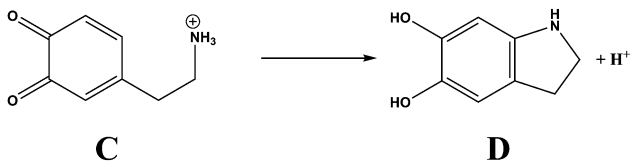

Scheme 2 Schematic representation of the oxidized dopamine cyclization reaction at pH = 7.4.[6]

follow-up dimerization.[14] This insight is readily appreciated since in the situation of an electrochemical quasi-reversible oxidation, both the forward (anodic) and backward (cathodic) processes contribute to the net current whilst the latter contribution is lost or diminished if the oxidation product is unstable and the species is lost on a timescale fast compared to electron transfer.

In the present paper, we study the mechanism and kinetics of dopamine oxidation around neutral pH where the follow-up kinetics is voltammetrically visible both in terms of the A/C voltammetric feature and the emergence of a new voltammetric feature attributed to the cyclization product.[15–24] The primary aim is to examine the effect of the follow-up kinetics on the voltammetric wave shape of the A/C process as recorded by Tafel analysis and investigate the dopamine oxidation mechanism at near-neutral pH. In particular it is shown that changing the voltammetric voltage scan rate leads to a marked change in the Tafel slope since at slower scan rates the loss of C in the voltammetric time scale is promoted with a decrease in the apparent reversibility of the A/C reaction. This provides a sensitive measure of the electron transfer kinetics and allows the conclusion to be drawn that the potential inversion mechanism operates at near-neutral pH. Moreover, the difference in the formal potentials, $\Delta E = E^0_{f,B/C} - E^0_{f,A/B}$ is shown to be consistent with the value obtained at pH = 0 and also independent of the electrode material so further validating the mechanism suggested.

Experimental

Chemicals and reagents

All reagents used were of analytical grade and acquired from Sigma-Aldrich (Gillingham, UK) and used without any further purification. All solutions were prepared using deionised water from Millipore (Watford, UK) with a measured resistivity of 18.2 MΩ cm at room temperature (298 K). All the buffers were prepared by dissoluing $NaHPO_4$ and Na_2HPO_4 in deionised water with a total concentration of 0.1 mol L^{-1} and pH = 7.4, resulting in a Phosphate Buffer Solution (PBS). The pH values were measured with a pH meter senseION pH 31 from Hach (Colorado, USA). Adjustments to pH were made by additions of

a 3 mol L^{-1} NaOH solution. To prevent the dopamine self-oxidation reaction, only fresh solutions were used and were degassed for 20 minutes prior each experiment using pure nitrogen from BOC Gases (Windlesham, UK) to prevent the atmospheric oxygen from oxidizing dopamine.

Electrochemical procedures

All electrochemical experiments were thermostatted at 25 ± 1 °C by a heat-stirrer UC 152 from Stuart (Stone, UK) and performed inside a Faraday cage. A μAutolab type III potentiostat/galvanostat from Metrohm (Utrecht, Netherlands) for all the electrochemical experiments. A three-electrode system was used with a Gold macroelectrode (GE) from BASi (West Lafayette, Indiana, USA) with an geometrical area of 0.0314 cm^2, operating as a working electrode, a pyrolytic graphite electrode from IJ Cambridge Scientific (Cambridge, UK) as the counter electrode and a saturated calomel electrode (SCE) ((+0.244 V *vs.* SHE) from BASi, Japan) as the reference electrode.

Cyclic voltammograms were performed by sweeping the potential from −0.1 V to +0.5 V, then from +0.5 to −0.5 V, and back to −0.1 V. The scan rates were used between 0.10 and 1.00 V s^{-1}. Before every experiment, the GE was polished using diamond spray suspensions with a decreasing particle size of 3.0, 1.0 and 0.1 μm from Kemet (Maidstone, UK) on a polishing pad from Buehler (Lake Bluff, Illinois, USA). All simulations were performed using the Digisim software from BASi (West Lafayette, Indiana, USA).[35,36]

Results and discussion

This section first presents voltammetric results for dopamine oxidation. These are then compared with the predictions of different Randles–Sevcik equations to give an initial indication of the mechanism of the A/C oxidation. Next, the follow-up reaction of C to D is explored. Full digital simulation is performed to extract kinetic and thermodynamic parameters especially in respect of the potential inversion and the rate of the follow-up cyclization reaction.

Cyclic voltammetry

Initially, cyclic voltammograms (CV) were recorded over a range of scan rates to overview the DA electrochemical behaviour. CVs were performed on a gold macroelectrode (GE) at near-neutral pH (7.4).

Representative experimental results are shown in Fig. 1. They show four electrochemical processes, an anodic (I) and a cathodic peak (II), which form a pair around 0.1 V. Another pair, a cathodic (III) and an anodic (IV) peak, around −0.3 V is also observed. The cathodic peak current of process (II) increased with an increase of the scan rate. The values of peak potentials and peak currents can be seen in Table S1 (ESI†). Moreover, the peak potentials of processes (I) and (II) shifted, to more positive and more negative potentials, respectively. Peaks (I) and (II) are associated with the A/C reaction, Scheme 1, whilst peaks III and IV are related to the oxidation

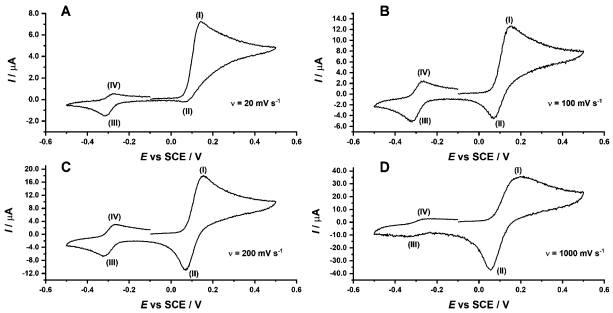

Fig. 1 CVs of DA solutions in PBS 0.1 M, pH = 7.4 at different scan rates: A = 0.02 V s^{-1}; B = 0.1 V s^{-1}; C = 0.20 V s^{-1} and D = 1.00 V s^{-1}.

of D, Scheme 2. The decrease in the size of peaks III and IV with the increase of the scan rate is consistent with the cyclization of D with a chemical reaction with a timescale corresponding to the voltage timescale used.

Randles–Sevcik equation and ECE mechanism analysis

The Randles–Sevcik equations are an analytical theoretical prediction of the peak currents of simple electrochemical process, for a reversible case, eqn (3), and for an irreversible one, eqn (4).

$$I_p = 0.446nFCA\sqrt{\frac{nFvD}{RT}} \quad (3)$$

$$I_p = 0.446\sqrt{n' + \beta}FCA\sqrt{\frac{nFvD}{RT}} \quad (4)$$

where I_p is the peak current in A, n is the overall number of electrons transferred, n' is the number of electrons prior to the rate determining step, F is the Faraday Constant in Coulomb mol^{-1}, C is the concentration in mol cm^{-3}, A the electrode area in cm^2, ν is the scan rate in V s^{-1}, R is the Gas Constant in J K^{-1} mol^{-1} and T is the temperature in K. A diffusion coefficient (D) of 7.7 × 10^{-6} cm s^{-1}, was obtained by chronoamperometry.[37]

Returning to Fig. 1, the A/C process was analysed in terms of a simple EE reaction. Specifically, the experimental results were compared to the theoretical predictions of the Randles–Sevcik equations. Fig. 2 shows the experimental peak currents for the oxidation A to C as a function of the square root of the voltage scan rate. Also shown are the theoretical predictions based in eqn (3) and (4) for the following-up cases: a simple reversible two-electron oxidation and an irreversible two-electron processes with either the first or the second step as the rate determining, assuming in each case a charge transfer coefficient of 0.5 in the rate determining step. It is clear that the high scan rate data fits with an overall two-electron process with the initial electron transfer as a rate determining hinting at a potential inversion mechanism but that there is a clear current enhancement over that predicted at lower scan rates.

In order to fully interpret the A/C voltammetry consideration has to be given to the follow-up reaction of C, as discussed in the next section and which explains the current enhancement seen at low scan rates.

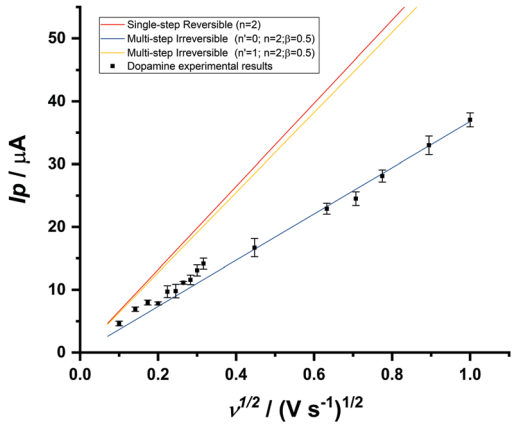

Fig. 2 Plot of the dopamine oxidative peak currents as a function of the square root of the scan rates, compared to the theoretical peak currents predicted by the Randles–Sevcik equations for a single step two-electron reversible transfer (–), for a multi-step irreversible (n' = 0; n = 2; β = 0.5) process (–), and for a multi-step irreversible (n' = 1; n = 2; β = 0.5) (–), together with experimental results (■). Electrode area = 0.0314 cm^2, C = 10^{-3} mol L^{-1}.

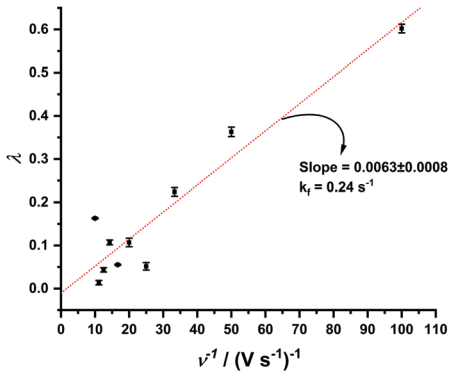

Fig. 3 Dimensionless parameter λ parameter *versus* the inverse of the voltage scan rate. Linear regression: $\lambda = 0.0063 \pm 0.0008\nu - 1 - 0.00873$. R^2 = 0.897.

An analysis of the DA oxidation as an EECEE process

We consider the following mechanism in which the product D can undergo oxidation at the potential of the A/C process:

$$\mathrm{A} \rightleftharpoons \mathrm{C} + 2\mathrm{e}^- \quad E^0_{f1} \tag{5}$$

$$\mathrm{C} \xrightarrow{k_f} \mathrm{D} \tag{6}$$

$$\mathrm{D} \rightleftharpoons \mathrm{F} + 2\mathrm{e}^- \quad E^0_{f2} \tag{7}$$

where E^0_f is the formal potential, k_f is the rate constant of formation of D from C. F is the oxidised cyclization product. The effective number of electrons transferred (n_{eff}) ($2 < n_{eff} < 4$), is a function of the dimensionless parameter (λ) where

$$\lambda = \left(\frac{RT}{F}\right)\frac{k_f}{\nu} \tag{8}$$

and the n_{app} values can be obtained by dividing the experimental peak current values by the theoretical prediction for a two-electron process (see above). The low scan rate data such as that shown in Fig. 2 were analyzed to give n_{app} values and then the published[38] working curve used to relate these to λ values. Then, a plot of λ, as inferred from the working curve against the reciprocal at the scan rate as suggested by eqn (9) was made and seen to be linear passing through the origin as shown in Fig. 4, which is consistent with the proposed EECEE mechanism. The slope of this plot allowed the interference of a value of k_f as approximately 0.2 s^{-1}, consistent with independent literature values[20,22] (Fig. 3). At this point the likely basic mechanism summarized in Schemes 1 and 2 has been identified, so attention was next turned to the full modelling of the voltammetry using Digisim as pioneered by Rudolph.[35,36]

Digisim simulations

Digisim software allows the simulation of voltammograms at macroelectrodes under linear diffusion conditions with various parameters describing the electrochemical and chemical steps. In the following, we use Digisim to fully model the experimental voltammetry of the DA system in the light of the

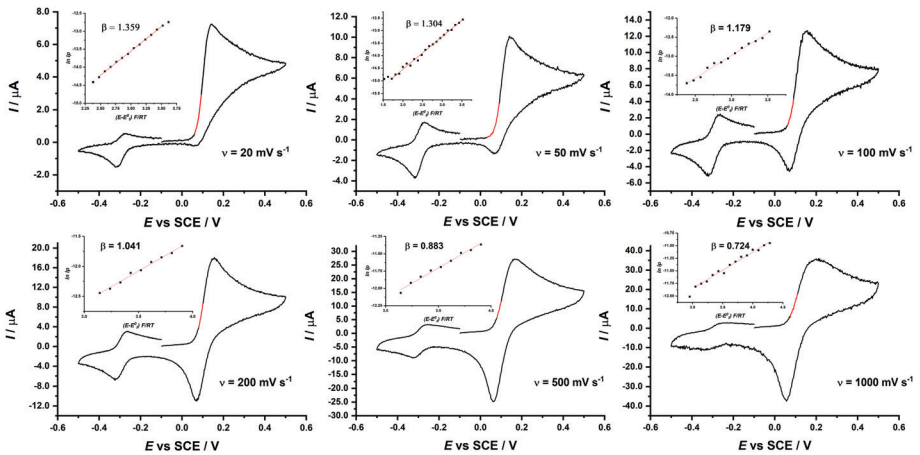

Fig. 4 CV presented in Fig. 1 with the respective Tafel plots as inset. The red parts of the voltammograms show the part of the curve sub-plotted to the Tafel analysis as in the insets. The parameters used in the simulations are presented in Table 5.

Table 3 β values obtained from the Tafel plots presented in Fig. 4 at different scan rates

ν/V s^{-1}	B values (experimental)
0.02	1.36 ± 0.01
0.05	1.30 ± 0.02
0.10	1.18 ± 0.03
0.20	1.04 ± 0.03
0.50	0.83 ± 0.03
1.00	0.72 ± 0.03

Table 4 Mechanistic steps used to simulate the DA system

Step order	Mechanism simulated	Correspondence	Type of step
1st	A − e$^-$ → B	(A/B)	Electrochemical
2nd	B − e$^-$ → C	(B/C)	Electrochemical
3rd	C → D	Cyclization(C/D)	Chemical
4th	D + 2e$^-$ → F	(D/E)	Electrochemical

Table 5 Optimized parameters for each simulated electrochemical and chemical step

Step	E_f^0/V	k^0/cm s^{-1}	D/cm^2 s^{-1}
A/B	0.2	0.025	7.7×10^{-6}
B/C	0.0	10^4 (reversible)	7.7×10^{-6}
D/E	−0.3	10^4 (reversible)	7.7×10^{-6}
E/F	−0.3	10^4 (reversible)	7.7×10^{-6}

Step	K	k_f/s^{-1}	k_b/s^{-1}
Cyclization (C/D)	10	0.2	0.02

K is the chemical step equilibrium constant, k_b is the homogeneous rate kinetics constant of the inverse reaction, k^0 is the standard electrochemical rate constant of the electron transfer.

preliminary analysis presented above paying particular attention to the A/C waveshapes and their associated Tafel slopes. In particular the anodic Tafel slope is given by

$$\beta = \frac{RT}{F}\frac{\mathrm{d}\ln I}{\mathrm{d}E} \quad (9)$$

provided that relatively little reactant concentration depletion taken place. In experimental practice, this constrains the analysis to the early part of a voltammetric peak, as shown in red, in Fig. 4, following the recommendations of Li *et al.*[39] Note that as defined by eqn (9), the Tafel slope is an experimental quantity independent of the overall number of electrons transferred in the oxidation.[40,41]

In order to probe the voltammetry of the dopamine oxidation system, Tafel plots were obtained from CVs presented in Fig. 1, these results are presented in Fig. 4.

The transfer coefficients values (β) obtained decreased systematically with the increase of the scan rate, Table 3, from 1.36 (20 mV s^{-1}) to 0.72 (1000 mV s^{-1}). This shift indicates a decrease in the apparent reversibility of the overall two-electron oxidation of A to C combined with the electrochemical of increased loss of C as the voltage timescale increases at slower scan rates. Thus, the decrease in reversibility is associated with the emergence of the D/F voltammetric feature. The outline mechanism used to interpret these data and informed by the discussion above can be summarised by means of the system given in Table 4. Each simulation was evaluated by comparing the peak currents, peak potentials, peak current ratios and the relation between the β values obtained from the Tafel plots regarding the scan rate between the simulated voltammograms and the experimental ones, to observe which mechanism better represents the latter.

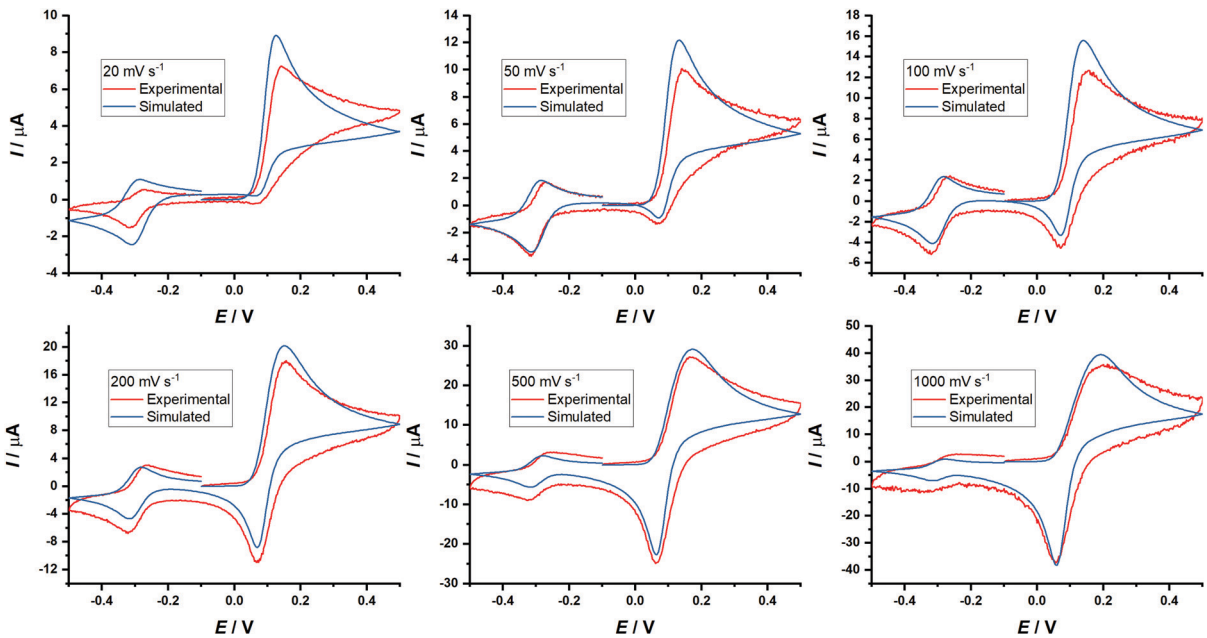

Fig. 5 (▬) Simulated CV voltammograms; (▬) of DA solutions in PBS 0.1 M, pH = 7.4 at different scan rates: A = 0.02 V s^{-1}; B = 0.05 V s^{-1}; C = 0.10 V s^{-1}; D = 0.20 V s^{-1}; E = 0.05 V s^{-1} and F = 1.00 V s^{-1}.

To fit the experimental waveshapes with the simulation, the homogeneous rate constant for step 3 and the parameters (E_f^0, k^0, and β) describing the electrochemical steps were varied and the resulting voltammograms were compared with the experimental ones. The optimized formal potential for A/B process was 0.2 V while the B/C was set at 0.0 V, following the reference presented by Lin *et al.*[1] which shows the potential inversion occurs before the chemical step. The cyclization (C/D) is a fast and irreversible reaction, as aforementioned. It affects the electrochemical steps at scan rates below 100 mV s^{-1}. The peak of the D/F couple was optimized by adding a slow homogeneous first order decomposition of F ($\sim 1\ s^{-1}$).

The best fit simulated voltammograms are shown in Fig. 5 superimposed on typical experimental data. Fig. 6 shows the successful fitting of the A/C voltammograms in terms of the ratio of the forward and reverse peak currents. A reasonable agreement is seen suggesting that several conclusions can be drawn. First and foremost the potential inversion mechanism operates at neutral pH consistent with the conclusion made under strongly acidic conditions.[1] Second, importantly, the simulations successfully reproduce the Tafel slopes and their variation with the voltage scan rate. Fig. 7 shows the level of agreement and indicates that concept of chemically induced electrochemical irreversibility in which the cyclization reaction exerts a profound influence on the Tafel slopes. Moreover, if this feature were neglected from the mechanistic analysis quite erroneous inferences the electrochemical kinetics of the A/C system would be drawn. Third, we note the oxidation product F show some slow kinetic lability on the voltammetric timescale.

In summary, the DA oxidation mechanism shown in Schemes 1 and 2 has been shown to be consistent with all the voltammetric data (Scheme 3).

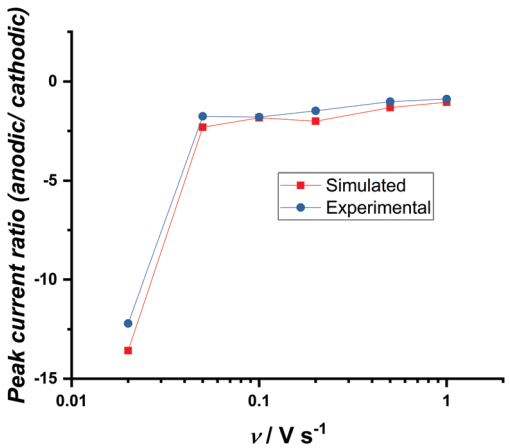

Fig. 6 Peak current ratios (anodic/cathodic) of the experimental and simulated voltammograms as a function of the scan rate, presented in a logarithm scale.

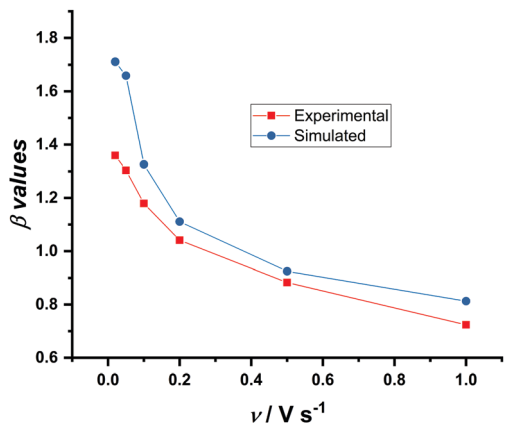

Fig. 7 β values for the A/C processes *versus* the scan rate.

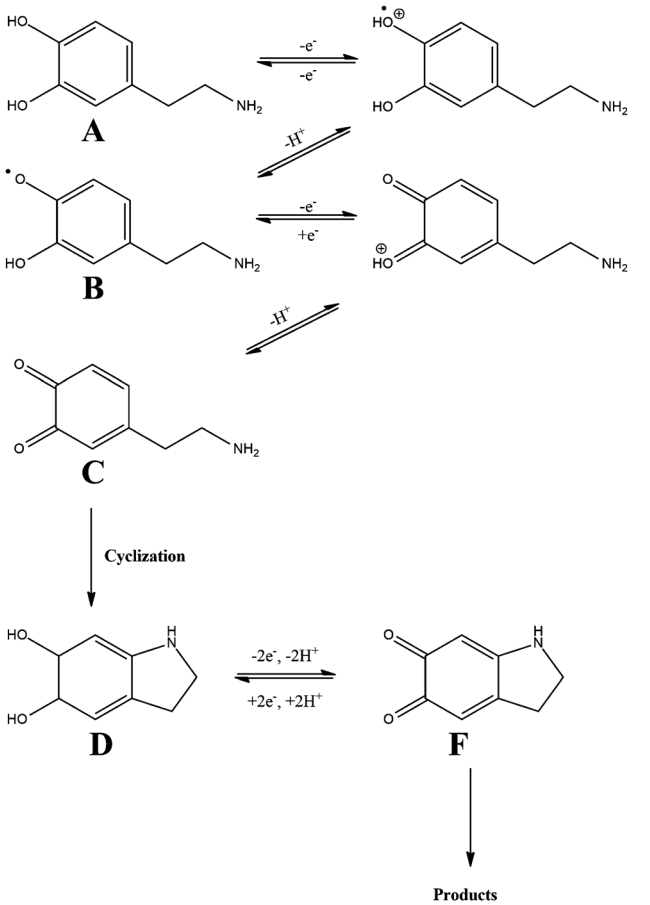

Scheme 3 Proposed electrochemical oxidation mechanism for dopamine in near-neutral pH.

Conclusions

Dopamine cyclization was studied at near-neutral pH in aqueous solution using cyclic voltammetry at gold microelectrodes and Digisim software used to digitally simulate the voltammograms. Dopamine oxidizes in a quasi-reversible process, A/C, involving two-electron transfers. The first one is a quasi-reversible transfer, which forms a semi-quinone (A/B) and the second one is a reversible one (B/C), forming a quinone. But, with a potential inversion such that B is more easily oxidized than A. The

electrochemical of the follow-up kinetics on the apparent reversibility of the A/C couple is profound as revealed by the Tafel slopes.

Conflicts of interest

The authors declare that there are no conflicts to declare.

Acknowledgements

The authors would like to thank the CAPES (Grant number PDSE 88881.187396/2018-01) and CNPq (Grant number 140833/2016-1) for the financial support of this work.

References

1 C. Lin, L. Chen, E. E. L. Tanner and R. G. Compton, Electroanalytical study of dopamine oxidation on carbon electrodes: from the macro- to the micro-scale, *Phys. Chem. Chem. Phys.*, 2018, **20**, 148–157.
2 Q. Lin, Q. Li, C. Batchelor-McAuley and R. G. Compton, Two-Electron, Two-Proton Oxidation of Catechol: Kinetics and Apparent Catalysis, *J. Phys. Chem. C*, 2015, **119**, 1489–1495.
3 D. H. Evans and K. Hu, Inverted potentials in two-electron processes in organic electrochemistry, *J. Chem. Soc., Faraday Trans.*, 1996, **92**, 3983.
4 C. E. Banks and R. G. Compton, *Understanding Voltammetry*, World Scientific Press Company, 3rd Ed., 2018.
5 J.-M. Savéant, *Elements of Molecular and Biomolecular Electrochemistry*, John Wiley & Sons, Inc., Hoboken, NJ, USA, 2006.
6 M. Salomäki, L. Marttila, H. Kivelä, T. Ouvinen and J. Lukkari, Effects of pH and Oxidants on the First Steps of Polydopamine Formation: A Thermodynamic Approach, *J. Phys. Chem. B*, 2018, **122**, 6314–6327.
7 B. J. Venton and R. M. Wightman, Psychoanalytical Electrochemistry: Dopamine and Behavior, *Anal. Chem.*, 2008, **75**, 414A–421A.
8 M. Shin, Y. Wang, J. R. Borgus and B. J. Venton, Electrochemistry at the Synapse, *Annu. Rev. Anal. Chem.*, 2019, **12**, 297–321.
9 E. Herlinger, R. F. Jameson and W. Linert, Spontaneous autoxidation of dopamine, *J. Chem. Soc., Perkin Trans. 2*, 1995, 259.
10 Q. Wei, F. Zhang, J. Li, B. Li and C. Zhao, Oxidant-induced dopamine polymerization for multifunctional coatings, *Polym. Chem.*, 2010, **1**, 1430–1433.
11 D. R. Dreyer, D. J. Miller, B. D. Freeman, D. R. Paul and C. W. Bielawski, Elucidating the Structure of Poly(dopamine), *Langmuir*, 2012, **28**, 6428–6435.
12 J. Liebscher, Chemistry of Polydopamine - Scope, Variation, and Limitation, *Eur. J. Org. Chem.*, 2019, 4976–4994.
13 N. Umek, B. Geršak, N. Vintar, M. Šoštarič and J. Mavri, Dopamine Autoxidation Is Controlled by Acidic pH, *Front. Mol. Neurosci.*, 2018, **11**, 1–8.
14 I. Streeter, S. F. Jenkinson, G. W. J. Fleet and R. G. Compton, Chemical instability promotes apparent electrochemical irreversibility: Studies on the electrode kinetics of the one electron reduction of the 2,6-diphenylpyrylium cation in acetonitrile solution, *J. Electroanal. Chem.*, 2007, **600**, 285–293.
15 M. D. Hawley, S. V. Tatawawadi, S. Piekarski and R. N. Adams, Electrochemical studies of the oxidation pathways of catecholamines, *J. Am. Chem. Soc.*, 1967, **89**, 447–450.
16 F. Zhang and G. Dryhurst, Oxidation Chemistry of Dopamine: Possible Insights into the Age-Dependent Loss of Dopaminergic Nigrostriatal Neurons, *Bioorg. Chem.*, 1993, **21**, 392–410.
17 G. Dryhurst, K. M. Kadish, F. Scheller and R. Renneberg, *Biological Electrochemistry*, Academic Press, London, 1st edn, 1982.
18 A. Brun and R. Rosset, Étude electrochimique de l'oxydation de la dihydroxy-3,4 phénylalanine (Dopa), *J. Electroanal. Chem. Interfacial Electrochem.*, 1974, **49**, 287–300.
19 S. Corona-Avendaño, G. Alarcón-Angeles, M. T. Ramírez-Silva, G. Rosquete-Pina, M. Romero-Romo and M. Palomar-Pardavé, On the electrochemistry of dopamine in aqueous solution. Part I: The role of [SDS] on the voltammetric behavior of dopamine on a carbon paste electrode, *J. Electroanal. Chem.*, 2007, **609**, 17–26.
20 D. C. S. Tse, R. L. McCreery and R. N. Adams, Potential oxidative pathways of brain catecholamines, *J. Med. Chem.*, 1976, **19**, 37–40.
21 T. E. Young and B. W. Babbitt, Electrochemical study of the oxidation of alpha-methyldopamine, alpha-methylnoradrenaline, and dopamine, *J. Org. Chem.*, 1983, **48**, 562–566.
22 A. W. Sternson, R. McCreery, B. Feinberg and R. N. Adams, Electrochemical studies of adrenergic neurotrans-mitters and related compounds, *J. Electroanal. Chem. Interfacial Electrochem.*, 1973, **46**, 313–321.
23 Y. Li, M. Liu, C. Xiang, Q. Xie and S. Yao, Electrochemical quartz crystal microbalance study on growth and property of the polymer deposit at gold electrodes during oxidation of dopamine in aqueous solutions, *Thin Solid Films*, 2006, **497**, 270–278.
24 X. Wen, Y.-H. Jia and Z.-L. Liu, Micellar effects on the electrochemistry of dopamine and its selective detection in the presence of ascorbic acid, *Talanta*, 1999, **50**, 1027–1033.
25 M. R. Deakin, P. M. Kovach, K. J. Stutts and R. M. Wightman, Heterogeneous mechanisms of the oxidation of catechols and ascorbic acid at carbon electrodes, *Anal. Chem.*, 1986, **58**, 1474–1480.
26 M. R. Deakin and R. M. Wightman, The kinetics of some substituted catechol/o-quinone couples at a carbon paste electrode, *J. Electroanal. Chem. Interfacial Electrochem.*, 1986, **206**, 167–177.
27 H. P. Hendrickson, A. D. Kaufman and C. E. Lunte, Electrochemistry of catechol-containing flavonoids, *J. Pharm. Biomed. Anal.*, 1994, **12**, 325–334.
28 L. Khalafi, M. Rafiee, M. Norouznia and Y. A. Asl, Electrochemical oxidation of catecholamines in the presence of aromatic amines: interplay between inter- and intramolecular nucleophilic addition, *Res. Chem. Intermed.*, 2015, **41**, 7151–7162.

29 A. Afkhami, D. Nematollahi, L. Khalafi and M. Rafiee, Kinetic study of the oxidation of some catecholamines by digital simulation of cyclic voltammograms, *Int. J. Chem. Kinet.*, 2005, **37**, 17–24.
30 E. L. Ciolkowski, K. M. Maness, P. S. Cahill, R. M. Wightman, D. H. Evans, B. Fosset and C. Amatore, Disproportionation During Electrooxidation of Catecholamines at Carbon-Fiber Microelectrodes, *Anal. Chem.*, 1994, **66**, 3611–3617.
31 S. Chumillas, T. Palomäki, M. Zhang, T. Laurila, V. Climent and J. M. Feliu, Analysis of catechol, 4-methylcatechol and dopamine electrochemical reactions on different substrate materials and pH conditions, *Electrochim. Acta*, 2018, **292**, 309–321.
32 R. P. da Silva, A. W. O. Lima and S. H. P. Serrano, Simultaneous voltammetric detection of ascorbic acid, dopamine and uric acid using a pyrolytic graphite electrode modified into dopamine solution, *Anal. Chim. Acta*, 2008, **612**, 89–98.
33 S. Schindler and T. Bechtold, Mechanistic insights into the electrochemical oxidation of dopamine by cyclic voltammetry, *J. Electroanal. Chem.*, 2019, **836**, 94–101.
34 D. Nematollahi and M. Rafiee, Electrochemical oxidation of catechols in the presence of acetylacetone, *J. Electroanal. Chem.*, 2004, **566**, 31–37.
35 M. Rudolph, A fast implicit finite difference algorithm for the digital simulation of electrochemical processes, *J. Electroanal. Chem. Interfacial Electrochem.*, 1991, **314**, 13–22.
36 M. Rudolph, Digital simulations with the fast implicit finite difference (FIFD) algorithm, *J. Electroanal. Chem.*, 1992, **338**, 85–98.
37 L. Chen, E. E. L. Tanner, C. Lin and R. G. Compton, Impact electrochemistry reveals that graphene nanoplatelets catalyse the oxidation of dopamine *via* adsorption, *Chem. Sci.*, 2018, **9**, 152–159.
38 I. Lavagnini, R. Antiochia and F. Magno, An extended method for the practical evaluation of the standard rate constant from cyclic voltammetric data, *Electroanalysis*, 2004, **16**, 505–506.
39 D. Li, C. Lin, C. Batchelor-McAuley, L. Chen and R. G. Compton, Tafel analysis in practice, *J. Electroanal. Chem.*, 2018, **826**, 117–124.
40 R. Guidelli, R. G. Compton, J. M. Feliu, E. Gileadi, J. Lipkowski, W. Schmickler and S. Trasatti, Definition of the transfer coefficient in electrochemistry (IUPAC Recommendations 2014), *Pure Appl. Chem.*, 2014, **86**, 259–262.
41 R. Guidelli, R. G. Compton, J. M. Feliu, E. Gileadi, J. Lipkowski, W. Schmickler and S. Trasatti, Defining the transfer coefficient in electrochemistry: An assessment (IUPAC Technical Report), *Pure Appl. Chem.*, 2014, **86**, 245–258.

